Periodic Heat Transfer Characteristics in a Square Channel with Various RVG Positions

Amnart Boonloi

Department of Mechanical Engineering Technology, College of Industrial Technology,
King Mongkut's University of Technology North Bangkok, Bangkok 10800, Thailand.
Email: amnartb [AT] kmutnb.ac.th

ABSTRACT—*This article, 3D numerical investigations on heat transfer behaviors and thermalperformance in a square channel with rib vortex generators (RVG) are presented. The effects of the RVGs with different gap ratio (g/H = 0 – 0.35) for the heat transfer profiles with constant blockage ratio (b/H, BR = 0.15), the pitch ratio (P/H, PR = 1) and flow attack angle ($\alpha = 30^o$) in an isothermal wall square channel are investigated for Reynolds number based on the hydraulic diameter of the square channel, Re = 100 – 1200. The SIMPLE algorithm and finite volume method (FVM) have applied for the computational domain. The mathematical results show that the RVGs with various positions produce the periodic profiles and the fully developed periodic profiles around the 2^{nd} module and 6^{th} – 9^{th} module, respectively. The use of the RVGs performs a higher heat transfer rate than the smooth channel with no RVG in all cases. The enhancement of the heat transfer rate is around 1 – 9 times over the smooth channel depended on the g/H values and Reynolds numbers. Additionally, the thermal enhancement factor, TEF, is found to be maximum around 4.05 at g/H = 0.10 and Re = 1200.*

Keywords— Forced convection, Heat transfer characteristics, Periodic Heat transfer, Rib, Vortex generators.

1. INTRODUCTION

The uses of the numerical method for heat transfer investigations in the heatingsystemshave been extensively seen in many engineering researches. The numerical method helps to save time, cost of materials and also human resources. Moreover, it can produce the visualizations of both flow structures and heat transfer characteristics that lead to the improvement method forthe new design of thecompact heat exchanger. However, the accuracies of the computational domain, boundary conditions and methodologies are very importantpart in this investigation.

The periodic concepts or periodic boundaries of the flow structure and heat transferbehaviors have been usually applied for the computational domain to save the time for investigation. The literature reviews on flow structure and heat transfer characteristicof the heating system with various generators, which using periodic concept for the computational domains are reported as Table 1.

Table 1: Literature reviews for the investigations by using periodic conditions.

Authors	Studied cases	Nu/Nu_0	f/f_0	TEF
Jedsadaratanachai et al.[1]	30^o inclined baffle Inline, two opposite walls, square channel BR = 0.2 PR = 0.5 – 2.5 Re = 100 – 2000	1 – 9.2	1 – 21.5	3.78
Kwankaomeng and Promvonge [2]	30^o inclined baffle One side, square channel BR = 0.1 – 0.5 PR = 1.0 – 2.0 Re = 100 – 1000	1 – 9.23	1.09 – 45.31	3.1
Promvonge et al. [3]	30^o inclined baffle	1.2 – 11.0	2 – 54	4

Authors	**Studied cases**	Nu/Nu_0	f/f_0	***TEF***
	Inline, two opposite walls, square channel *BR* = 0.1 – 0.3 *PR* = 1.0 – 2.0 *Re* = 100 – 2000			
Promvonge and Kwankaomeng [4]	45^o V–baffle Staggered, two opposite walls, *AR* = 2 channel *BR* = 0.05 – 0.3 *PR* = 1.0 *Re* = 100 – 1200	1 – 11	2 – 90	2.75
Promvonge et al. [5]	45^o inclined baffle Inline – staggered, two opposite walls, square channel *BR* = 0.05 – 0.3 *PR* = 1.0 *Re* = 100 – 1000	1.5 – 8.5	2 – 70	2.6
Promvonge et al. [6]	45^o V–baffle Inline Downstream, two opposite walls, square channel *BR* = 0.1 – 0.3 *PR* = 1.0 – 2.0 *Re* = 100 – 2000	1 – 21	1.1 – 225	3.8
Boonloi [7]	20^o V–baffle Inline Downstream- Upstream, two opposite walls, square channel *BR* = 0.1 – 0.3 *PR* = 1.0 *Re* = 100 – 2000	1 – 13	1 – 52	4.2
Boonloi and Jedsadaratanachai [8]	30^o V–baffle Downstream, One side, square channel *BR* = 0.1 – 0.5 *PR* = 1.0 – 2.0 *Re* = 100 – 1200	1 – 14.49	2.18 – 313.24	2.44

The periodic concepts were reported by Jedsadaratanachai et al. [9] and Promvonge et al. [10]. Jedsadaratanachai et al. [9] studied the flow behavior in a circular tube with baffles. They found that the flow profiles in the tube perform periodic patternsaround the 2nd module and become to fully developed periodic flow profiles at about *x*/*D* = 7 downstream of the inlet. Promvonge et al. [10] numerical investigated the periodic turbulent flow in a square duct. They explained that the flowprofilesbecome to fully developed periodic flow and heat transfer profiles at about *x*/*D* = 7–11 downstream of the entry region. According to the *Ref*s. [1, 9 and 10], the speed rate of the fully developed periodic flow and heat transfer wasreported. The increasing *BR*, *Re*and reducing *PR*are factors for the speedup rate of the fully developed periodic flow and heat transfer in the test channel. Jedsadaratanachai [11] investigated the periodic flow

profiles in a square channel with variouspositions of the vortex generators. The periodic flow profiles appear around the 2nd module and the fully developed periodic flow profiles show around 6th – 9th module, whichare concluded by Jedsadaratanachai [11].

As the *Ref*. [11], the influences of the position for rib vortex generators on heat transfer characteristics, thermal performance and the appearance of the periodic heat transfer profiles have rarely been reported. Therefore, this work focuses on the heat transfer behavior in an isothermal wall square channel with variousthe positions of the rib vortex generators (*RVG*). The different gap ratios, g/H = 0 – 0.35, for α = 30^o inclined rib vortex generator, with constant *BR* = 0.15 and *PR* = 1.00 are studied numerically for *Re* = 100 – 1200.

2. MATHEMATICAL FOUNDATION, BOUNDARY CONDITION AND ASSUMPTION

The computational domain, grid system of the computational domain and parameters are referred as *Ref*s. [9, 11]. The boundary conditions of the currentcomputational domain are displayed as Table 2, while the assumptions for present investigation are as follows:

- Steady state in three–dimensions.
- The flow is laminar and incompressible.
- Constant fluid properties.
- Body forces and viscous dissipation are ignored.
- Negligible radiation heat transfer.

Table 2: Boundary conditions of the computational domain.

Zone	Boundary condition
Square channel walls	Constant temperature at 310 K No slip wall condition
*RVG*s	Adiabatic wall condition
Inlet	Periodic condition Constant mass flow rate of the air at 300K
Outlet	Periodic condition

Based on the assumptions, the channel flow is governed by the continuity, the Navier–Stokes equations and the energy equation. In the Cartesian tensor form these equations can be written as follows:

Continuity equation:

$$\frac{\partial}{\partial x_i}(\rho u_i) = 0 \tag{1}$$

Momentum equation:

$$\frac{\partial(\rho u_i u_j)}{\partial x_j} = -\frac{\partial p}{\partial x_i} + \frac{\partial}{\partial x_j}\left[\mu\left(\frac{\partial u_i}{\partial x_j} + \frac{\partial u_j}{\partial x_i}\right)\right] \tag{2}$$

Energy equation:

$$\frac{\partial}{\partial x_i}(\rho u_i T) = \frac{\partial}{\partial x_j}\left(\Gamma \frac{\partial T}{\partial x_j}\right) \tag{3}$$

where, Γ is the thermal diffusivity.

$$\Gamma = \frac{\mu}{\Pr} \quad (4)$$

The solutions are measured to be converged when the normalized resi-dual values are less than $10^{-9}$for for the energy equation.

The Reynolds number is defined as:

$$\mathrm{Re} = \rho \bar{u} D_h / \mu \quad (5)$$

The heat transfer is measured by the local Nusselt number which can be written as

$$Nu_x = \frac{h_x D}{k} \quad (6)$$

The average Nusselt number can be obtained by

$$Nu = \frac{1}{A} \int Nu_x \partial A \quad (7)$$

The friction factor, f is computed by pressure drop, Δp as

$$f = \frac{(\Delta p / P) D}{\frac{1}{2} \rho \bar{u}^2} \quad (8)$$

The thermal enhancement factor (*TEF*) is defined as the ratio of the heat transfer coefficient of an augmented surface, h to that of a smooth surface, h_0, at an equal pumping power and given by

$$TEF = \left. \frac{h}{h_0} \right|_{pp} = \left. \frac{Nu}{Nu_0} \right|_{pp} = (Nu/Nu_0)/(f/f_0)^{1/3} \quad (9)$$

Where, Nu_0 and f_0 stand for Nusselt number and friction factor for the smooth square channel, respectively.

3. SQUARE CHANNEL GEOMETRY AND COMPUTATIONAL DOMAIN

From *Ref.* [11], Figs. 1*a*, *b*, *c* and *d* show a square channel insertedwith *RVG*s, details of the test section, computational domain and cross sectional area in y-x axis, respectively. The 30°*RVG*s are organized with inline arrangementand placed on both the upper and lower parts of the channel. In the test channel, the air enters at an inlet temperature, T_{in} and flows over *RVG*s where *b* is the *RVG*s height, *H* set to 0.05 m, is the channel height and *b*/*H*is known as the blockage ratio, *BR* = 0.15. The longitudinal distance between the *RVG*s is set to *P*, which *P*/*H*is defined as the pitch ratio, *PR* = 1.0. The positions of *RVG*s are varied by considering the distance between the upper/lower walls of the square channel to the *RVG*s, *g*, and *g*/*H* is identified as the gap ratio. The gap ratios are varied in a range of *g*/*H* = 0 – 0.35 in the present study.Due to the numerical results in part of a grid independent test show that the augmentation of grid cell from 125,500 to 180,000 has no effect for both heat transfer rate and friction loss, therefore, the 125,500 hexahedral cellsareused for the present computational domain.

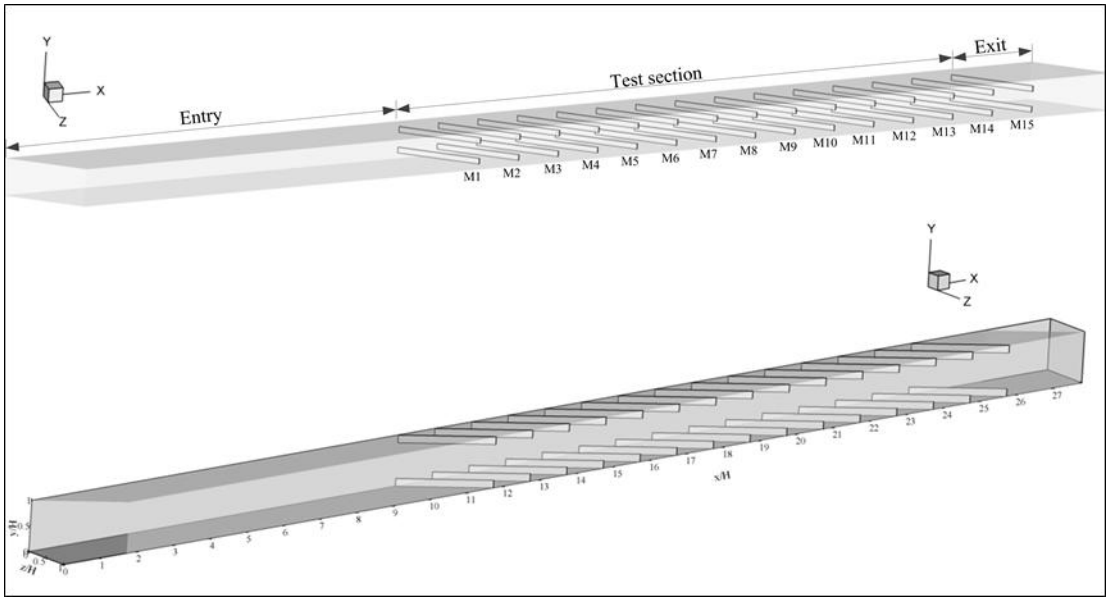
Y
X
Z
Entry
Test section
Exit
M1
M2
M3
M4
M5
M6
M7
M8
M9
M10
M11
M12
M13
M14
M15

(a)

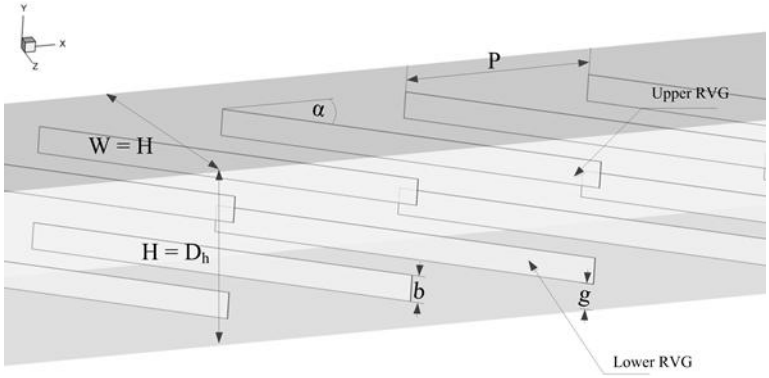
Y
X
Z
P
α
W = H
H = Dh
b
g
Upper RVG
Lower RVG

(b)

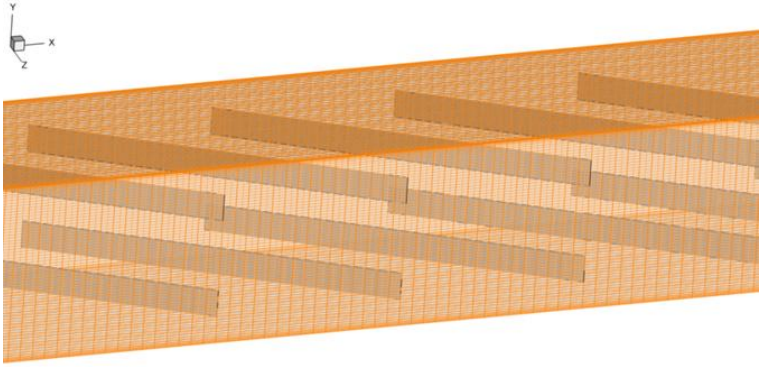
Y
X
Z

(c)

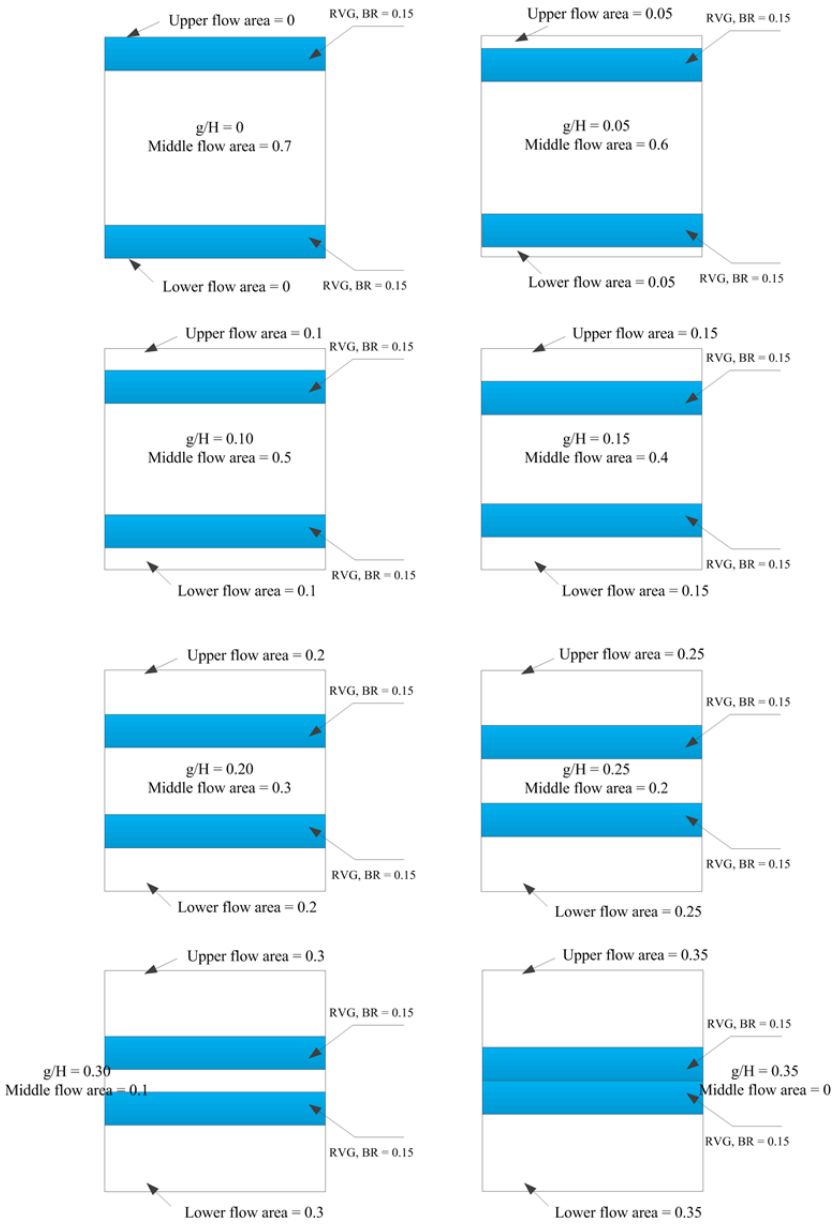

(d)

Figure 1:(a) square channel with *RVG*s, (b) details of square channel with *RVG*s, (c) computational domain, and (d) cross sectional area in y-z axis for *RVG*s [11]

4. RESULTS AND DISCUSSION

4.1Verification of the smooth square channel

The verification of the heat transfer in the smooth square channel with no *RVG* is presented in the Fig. 2. The comparison between the present prediction and the correlation of the Nusselt number [12] is found to be in good agreement within±0.04% deviationof all Reynolds number values. The exact solution of the Nusselt number for laminar flows in thesquare channel with constant wall temperature is shown in equation 8.

$Nu_0 = 2.98$ (8)

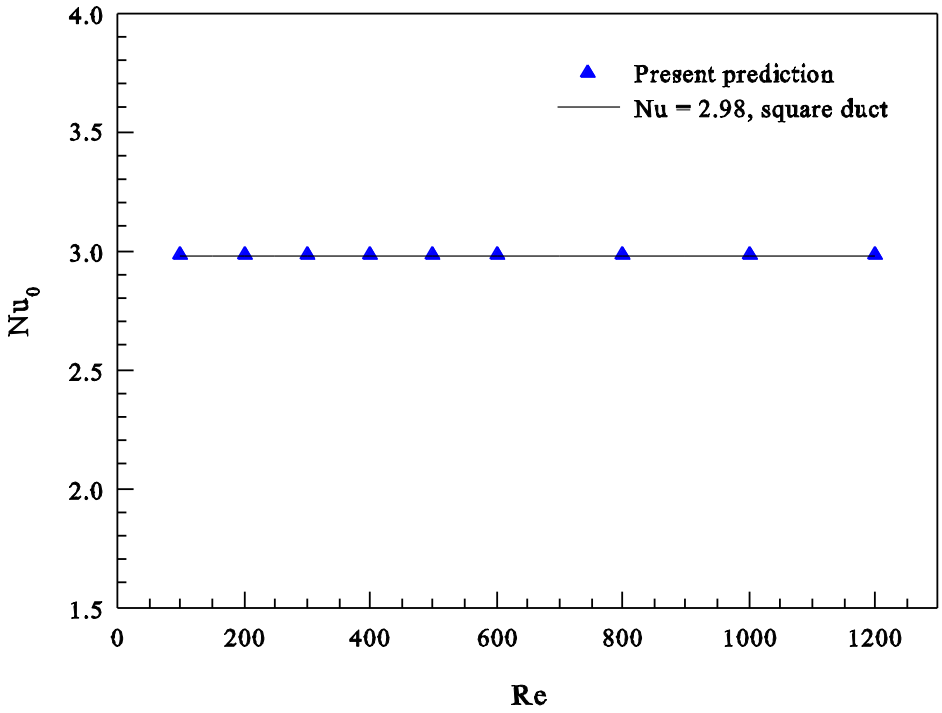

Figure 2: Validation of the Nusselt number for smooth channel

4.2 Periodic heat transfer profiles

The periodic heat transfer profiles for various g/H values are presented in term of Nu_x contours on the channel walls; rib leading edge (*RLE*) sidewall, rib trailing edge (*RTE*) sidewall and the upper wall (due to the symmetry part of the upper–lower parts of the channel) of the test section as depicted in Figs. 3, 4, 5, 6, 7, 8, 9 and 10 for g/H = 0, 0.05, 0.10, 0.15, 0.20, 0.25, 0.30 and 0.35, respectively, atRe = 800. As seen in the figures, The heat transfer profiles can be divided as two groups: developing heat transfer characteristics and periodic heat transfer behaviors. In general, the developing heat transfer characteristics are found in the earlier regime of the test section, after that the heat transfer behaviors develop into periodic patterns when passing around 6^{th} – 9^{th} module depended on g/H values.

Atg/H = 0, the developing heat transfer profiles are found around 1^{st} – 9^{th} module, and then become to the periodic heat transfer profiles for all sides of the channel walls. Similar trends are found atg/H = 0.05. The periodic profiles of heat transfer perform faster when increasing g/H values as seen in case g/H = 0.10, which the periodic heat transfer profiles are appearing around the 6^{th} module of the test section.

In rangeg/H = 0.15 – 0.30, the 3^{th} – 5^{th} module on both the *RTE* and *RLE* sidewalls perform periodic heat transfer profiles, while the upper walls show periodic heat transfer profiles slower than *RLE* and *RTE* sidewalls. The periodic heat transfer profiles at the upper walls appear around the 9^{th} module forg/H = 0.15 – 0.25 and around the 5^{th} module for g/H = 0.30.

The g/H = 0.35, the profiles of periodic heat transfer appear at 12^{th} – 13^{th} module of all the channel walls. It can be concluded that the g/H = 0.35 provides the slowest periodic heat transfer profiles in comparison with the other cases.

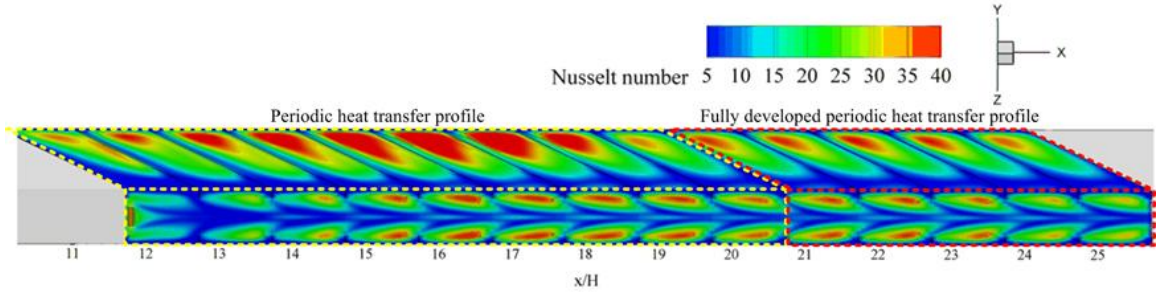

(a)

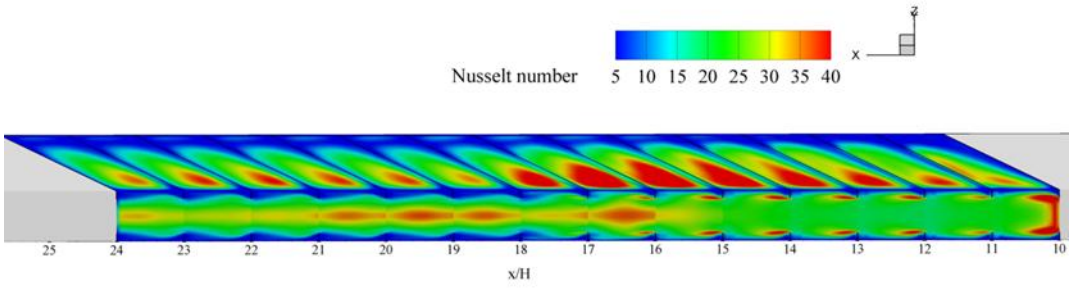

(b)

Figure 3: Contours of Nu_x for (a)upper wall and *RTE* sidewall, and (b)upper wall and *RLE* sidewall at $g/H = 0$ and $Re = 800$.

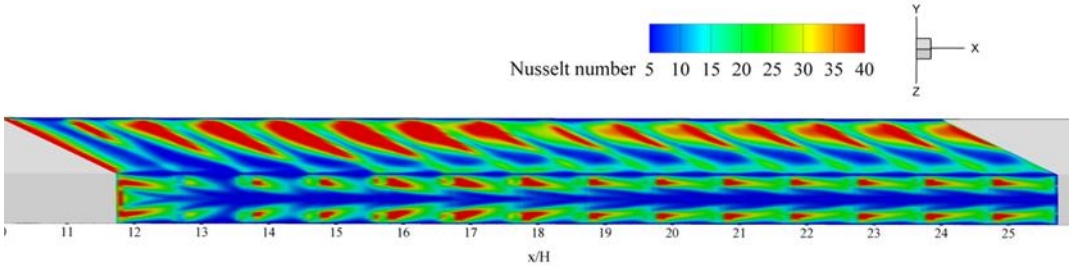

(a)

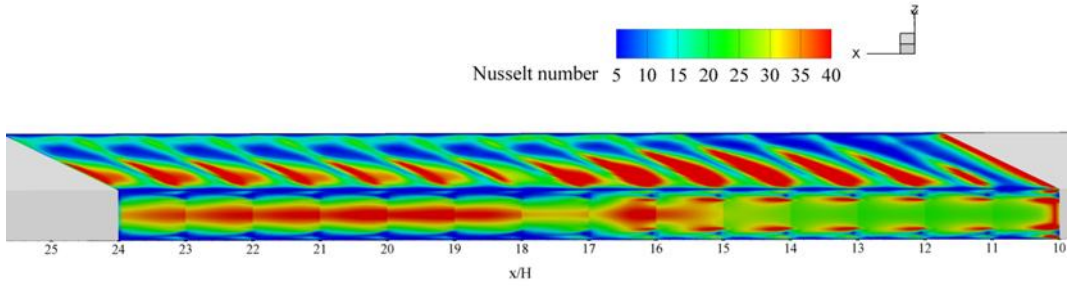

(b)

Figure 4: Contours of Nu_x for (a)upper wall and *RTE* sidewall, and (b)upper wall and *RLE* sidewall at $g/H = 0.05$ and $Re = 800$.

In addition, the distances between the *RVG* and the upper-lower walls of the channel or gap ratio have effect for the periodic heat transfer profile. Except for $g/H = 0.35$, the rising g/H values lead to the speed up on the periodic heat transfer characteristics on the *RLE* and *RTE* sidewalls, while the periodic heat transfer profiles in the upper–lower walls of the channel give general trend, which becomes to periodic heat transfer profiles around 8^{th} – 9^{th} module.

According to the above results, the Nu_x contours of the channel walls can divided into two regimes for all cases; the developing heat transfer profiles and the periodic heat transfer profiles. The Nu_x contours can roughly conclude the heat transfer behavior for similar profiles or not, but cannot identify the values of heat transfer in the test channel. Therefore, the variations on Nu/Nu_0 of the channel walls with various *RVG*positions are presented in the next topic to describe the details of the periodic heat transfer profiles and also comparing the heat transfer values in the form of the *Nu*.

4.3 Variations of Nu/Nu_0 with various positions

The variations of the Nu/Nu_0 with various x/H, y/H and z/H positions for the *RVG* in the square channel are presented in the Figs. 11, 12, 13, 14, 15, 16, 17 and 18 for $g/H = 0$, 0.05, 0.10, 0.15, 0.20, 0.25, 0.30 and 0.35, respectively, at $Re = 800$. The values of Nu/Nu_0 are presented for *RLE* sidewall ($z/H = 0$), *RTE* sidewall ($z/H = 1$) and lower wall ($y/H = 0$) of the square channel for all cases. In general, the numerical results in term of Nu/Nu_0 with various positions can be divided into two characteristics: the periodic heat transfer profiles and the fully developed periodic heat transfer profilessimilarly as the heat transfer characteristics, which are presented in the previous part. The periodic heat transfer profiles mean that the Nu/Nu_0 values perform similar profiles, but

differences in the values, while the fully developed periodic heat transfer profiles mean that on both the values and the profile of the Nu/Nu_0 provide similarly.

The variations of Nu/Nu_0 forg/H = 0, which has no gap between *RVG* and the upper–lower walls are presented as Fig. 11. It is found that the periodic heat transfer profiles appear around the 2nd module and become to the fully developed periodic heat transfer profile at 6th – 9th module for all positions. The rate for the apparent on both periodic heat transfer and fully developed periodic heat transfer of all positions are seen to be equivalent. Similar results are found in Fig. 12 for g/H = 0.05.

The faster rate to become to the fully developed periodic heat transfer is found at g/H = 0.10, which the fully developed periodic heat transfer profiles show around 5th – 8th module. It is noted that the lower wall of the channel seems to be slowly rate to become to the fully developed periodic heat transfer profiles in comparison with *RLE* and *RTE* sidewalls.

The g/H = 0.15 – 0.30, the fully developed periodic heat transfer profiles at the *RLE* and *RTE* sidewalls perform faster, while the lower wall of the test section is not found as the fully periodic heat transfer profiles. This means that the gap between *RVG* and the lower wall of the test section is an important factor for heat transfer behavior. The periodic heat transfer profiles are seen atg/H = 0.35, but the fully developed periodic heat transfer profiles do not appear in this case.

The periodic heat transfer profiles and the fully developed periodic heat transfer profiles are appearing depended on the gap ratio of the *RVG*. The g/H values, which decrease the continuous flow areas (g/H = 0.15 – 0.30) lead to become to the fully developed periodic heat transfer behaviors faster on both sidewalls of the channel, while the reversed results are found in the upper–lower walls of the test section.

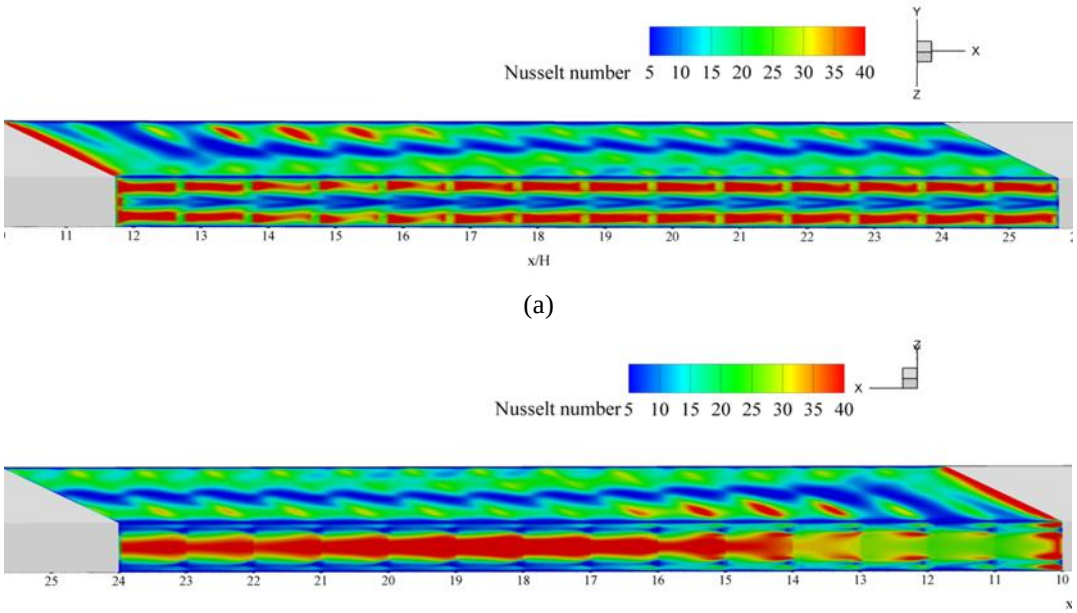

Figure 5: Contours of Nu_x for (a) upper wall and *RTE* sidewall, and (b) upper wall and *RLE* sidewall at g/H = 0.10 and *Re* = 800.

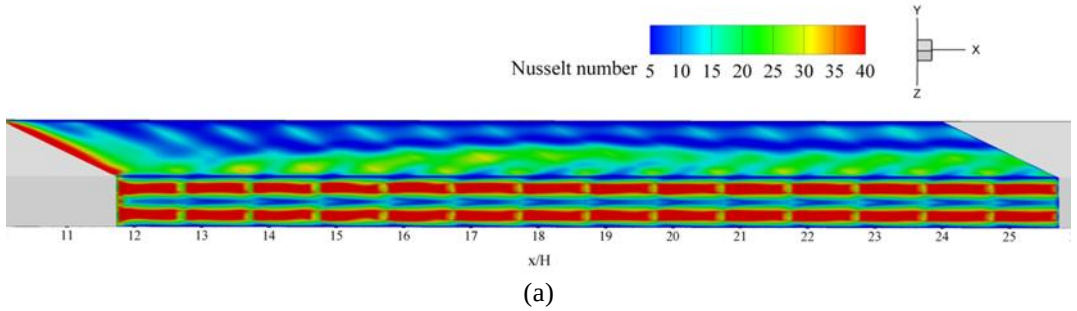

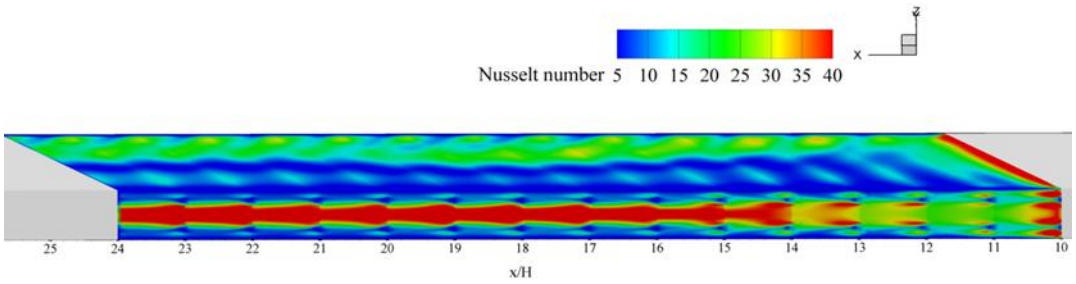

(b)

Figure 6: Contours of Nu_x for (a) upper wall and *RTE* sidewall, and (b) upper wall and *RLE* sidewall at g/H = 0.15 and *Re* = 800.

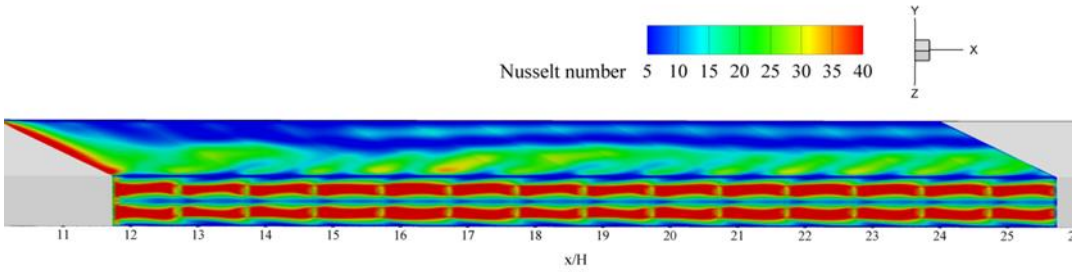

(a)

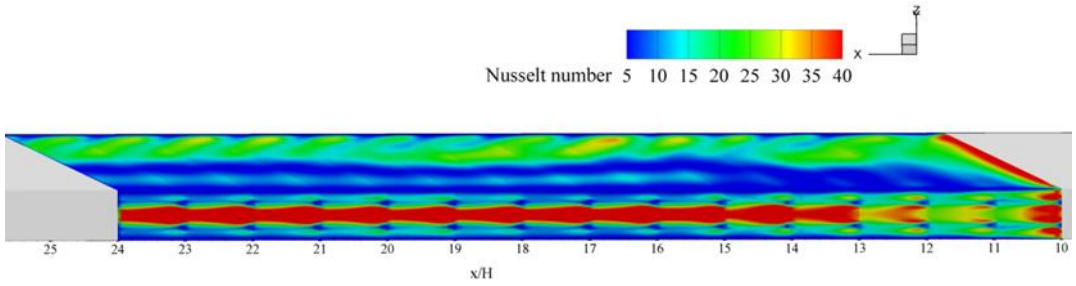

(b)

Figure 7: Contours of Nu_x for (a) upper wall and *RTE* sidewall, and (b) upper wall and *RLE* sidewall at g/H = 0.20 and *Re* = 800.

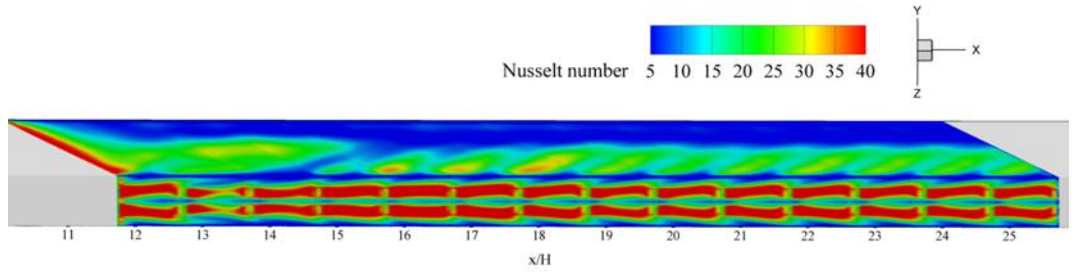

(a)

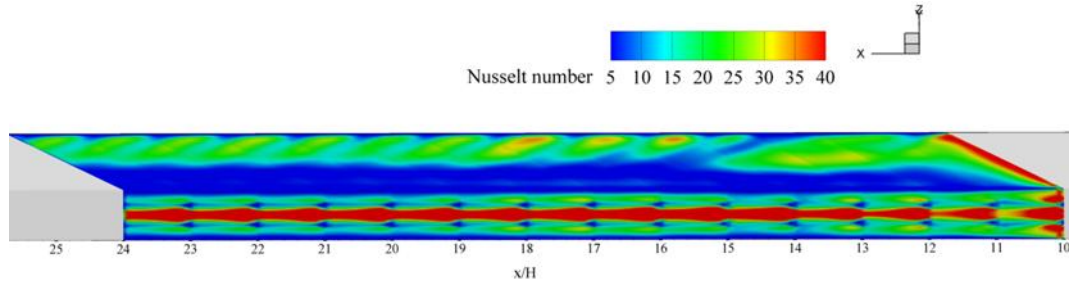

(b)

Figure 8: Contours of Nu_x for (a) upper wall and *RTE* sidewall, and (b) upper wall and *RLE* sidewall at g/H = 0.25 and *Re* = 800.

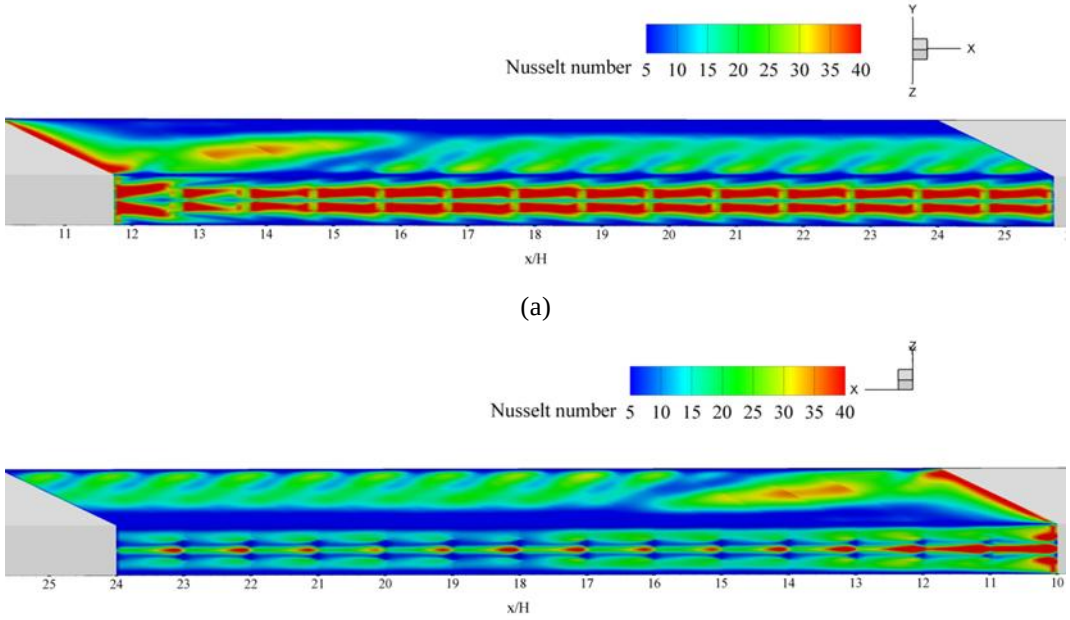

Figure 9: Contours of Nu_x for (a) upper wall and *RTE* sidewall, and (b) upper wall and *RLE* sidewall at g/H = 0.30 and *Re* = 800.

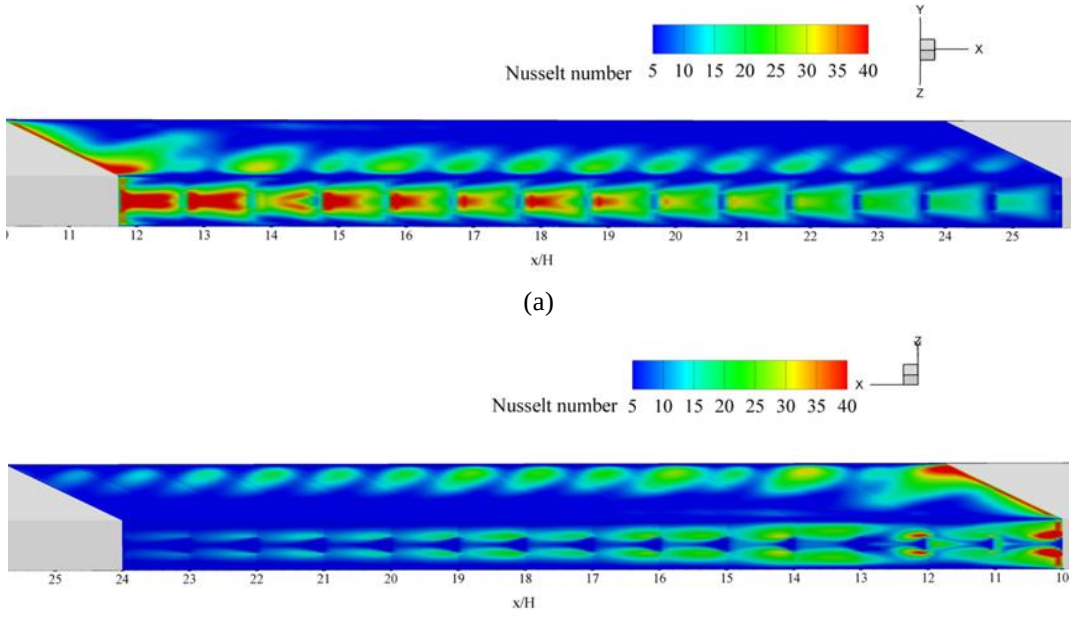

Figure 10: Contours of Nu_x for (a) upper wall and *RTE* sidewall, and (b) upper wall and *RLE* sidewall at g/H = 0.35 and *Re* = 800.

4.4 Relationship of flow structure and heat transfer

The plots of the streamlines impinging jet on the walls with Nu_x contours of the channel are presented as Figs. 19*a*, *b* and *c* for g/H = 0, 0.05 and 0.10, respectively. According to *Ref.* [11], the g/H = 0 produces the impinging jets on the *RLE* sidewall and on the lower wall of the channel. The impinging regimes are found in case of g/H = 0.05 and the penetration for some part of the fluid flowis appearing on the lower part that close to the lower wall. The fluid flows through the lower part of *RVG* are also seen as g/H = 0.10 that lead to the decreasing heat transfer on the lower wall of the test section.

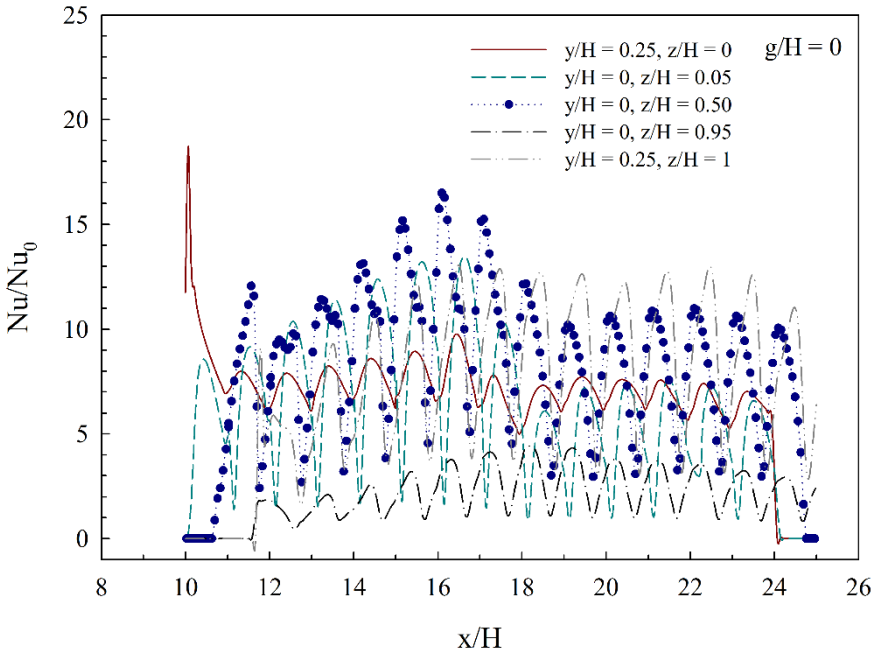

Figure 11: The variations of Nu/Nu_0 with x/H at various y/H and z/H for g/H = 0 and Re = 800.

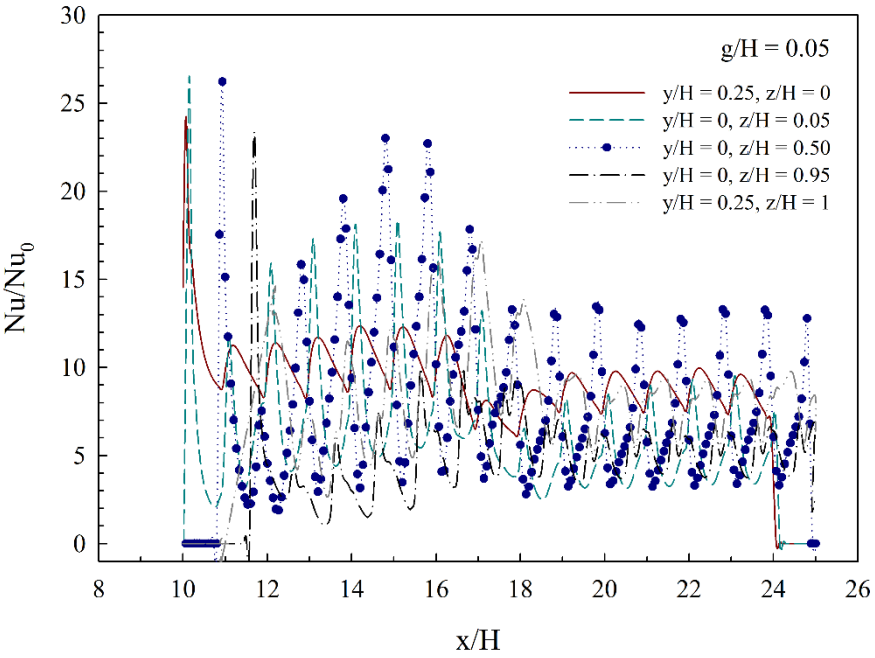

Figure 12: The variations of Nu/Nu_0 with x/H at various y/H and z/H for g/H = 0.05 and Re = 800.

4.5 Performance evaluation

The performance evaluations for the square channel with *RVG*s are presented for heat transfer, friction factor and thermal performance in terms of the Nusselt number ratio (Nu/Nu_0), the friction factor ratio (f/f_0) and the thermal enhancement factor (*TEF*), respectively. The use of the *RVG*s performs higher heat transfer rate, friction loss and the thermal enhancement factor higher than the smooth channel for all g/H values.

The variations of the Nu/Nu_0 with the Reynolds number are displayed as the Fig. 20. The Nu/Nu_0 tends to increase with the rise of Reynolds number for all cases. The Nu/Nu_0 is found to be around 1 – 9 depended on g/H values and Reynolds numbers. The maximum Nu/Nu_0 is found at g/H = 0.10 and Re = 1200 around 9.

Fig. 21 presents the variations of the f/f_0 with the Reynolds number. It is found that the f/f_0increases with the rise of Reynolds number for all cases. The enhancement of the f/f_0 is around 1.5 – 11.2 depended on g/H values and the Reynolds number.

The variations of the *TEF* with the Reynolds number are presented in Fig. 22. The *TEF*varies between 1 – 4.05 depended on *Re* and g/H values. The optimum *TEF* is found at g/H = 0.10 at the highest Reynolds number, *Re* = 1200, around 4.05.

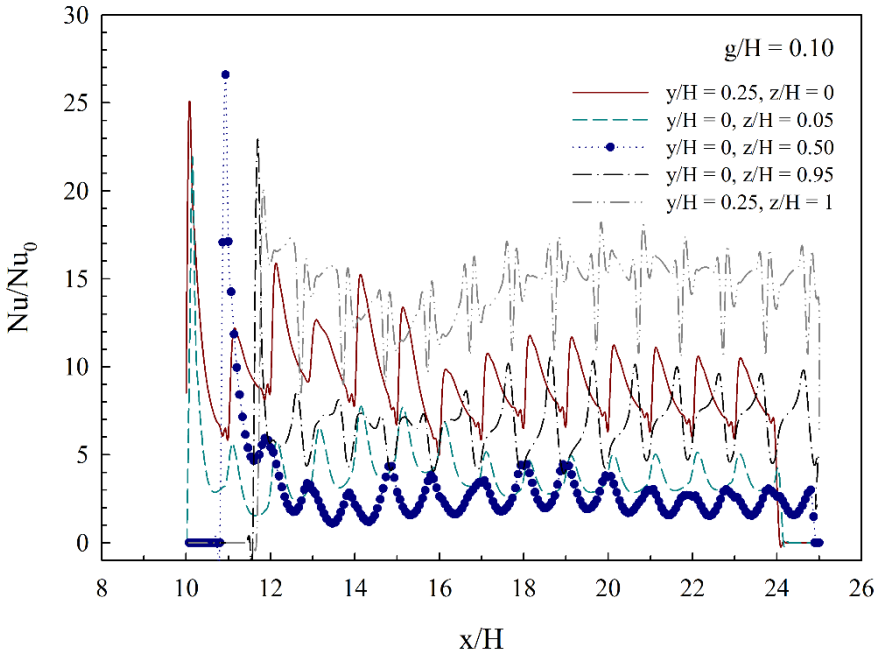

Figure 13: The variations of Nu/Nu_0 with x/H at various y/H and z/H for g/H = 0.10 and *Re* = 800.

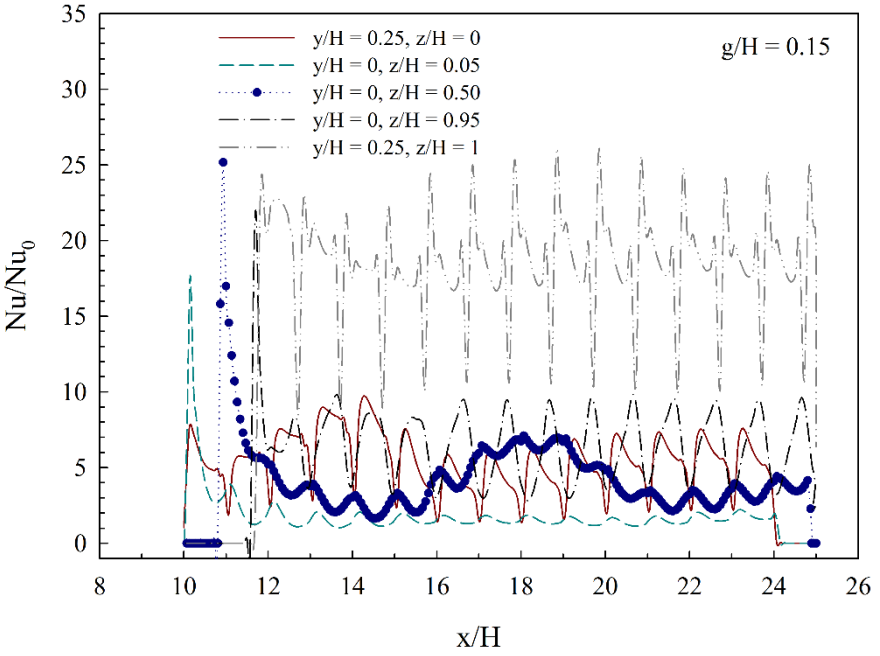

Figure 14: The variations of Nu/Nu_0 with x/H at various y/H and z/H for g/H = 0.15 and *Re* = 800.

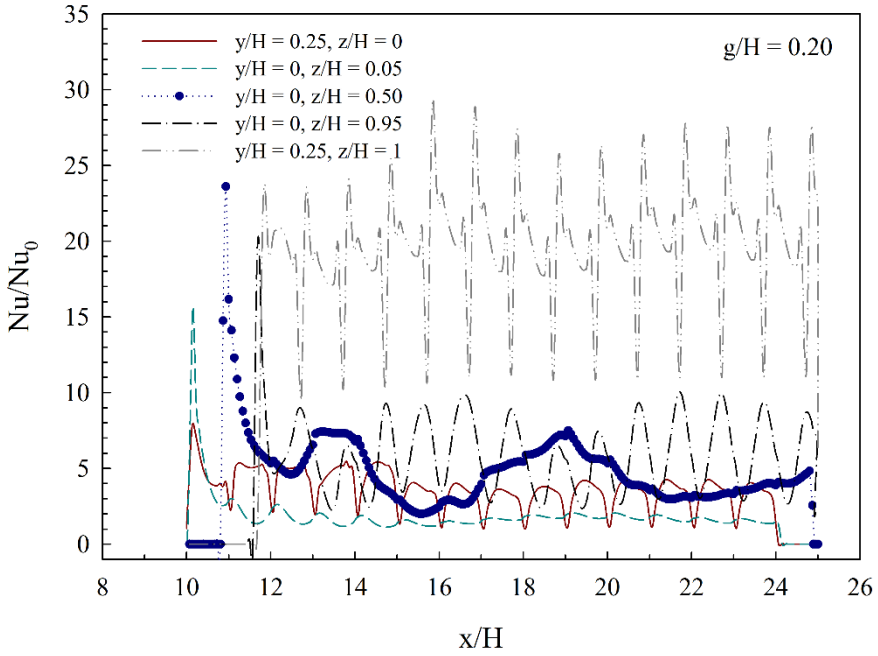

Figure 15: The variations of Nu/Nu_0 with x/H at various y/H and z/H for g/H = 0.20 and Re = 800.

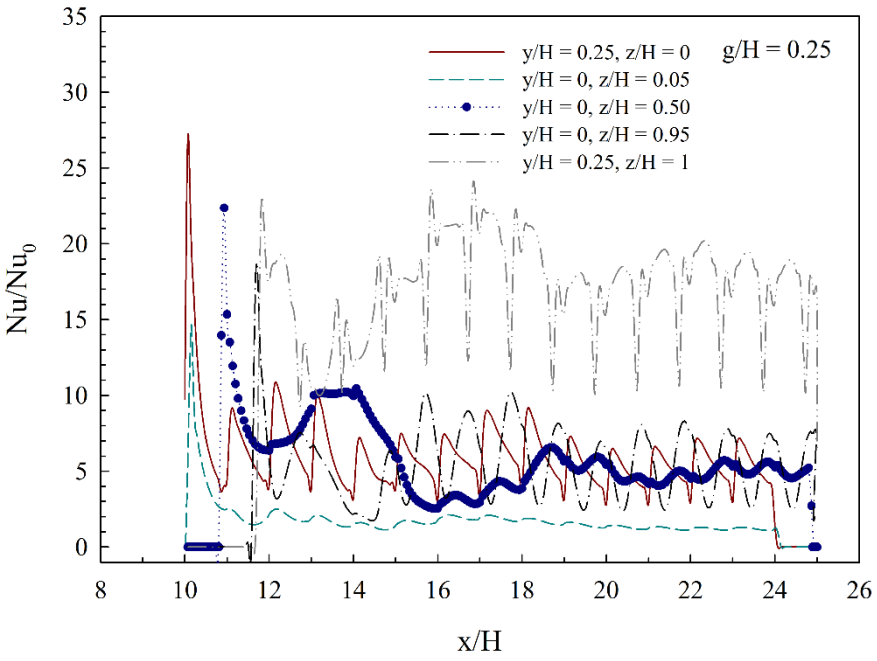

Figure 16: The variations of Nu/Nu_0 with x/H at various y/H and z/H for g/H = 0.25 and Re = 800.

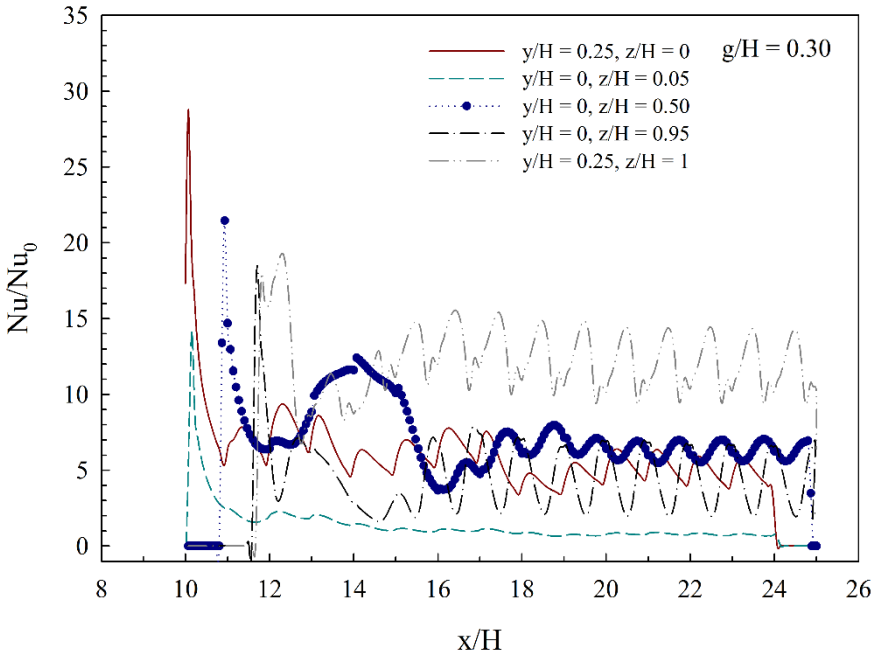

Figure 17: The variations of Nu/Nu_0 with x/H at various y/H and z/H for g/H = 0.30 and Re = 800.

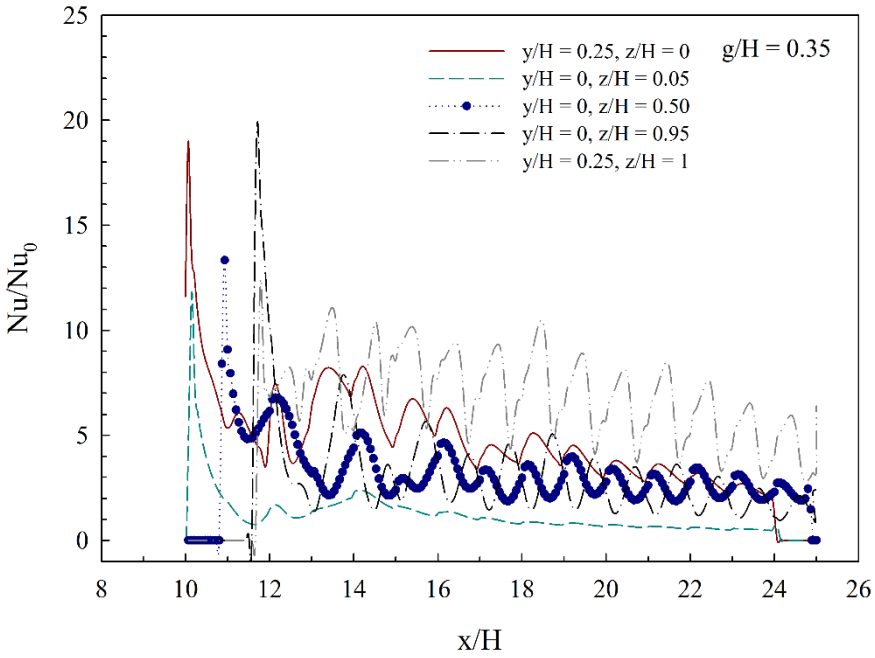

Figure 18: The variations of Nu/Nu_0 with x/H at various y/H and z/H for g/H = 0.35 and Re = 800.

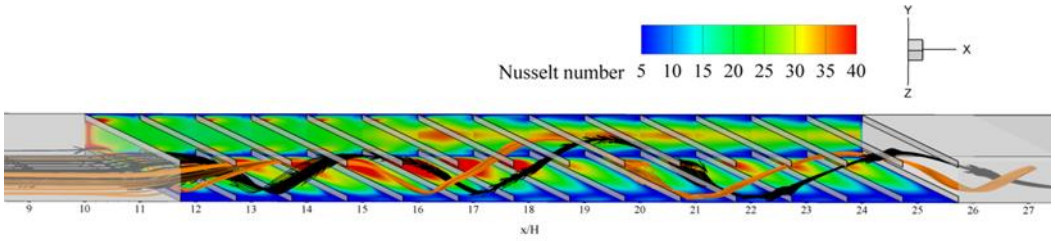

(a)

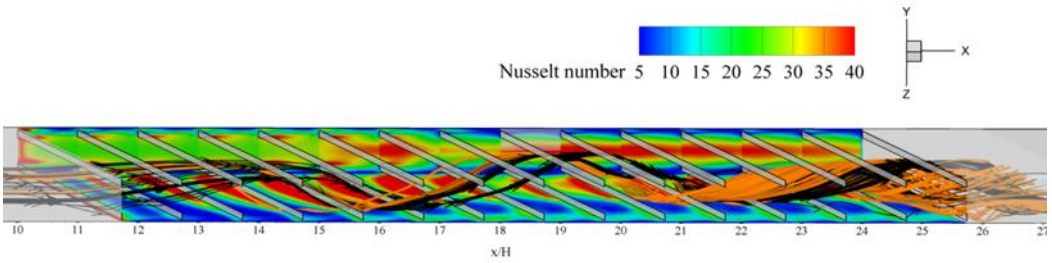

(b)

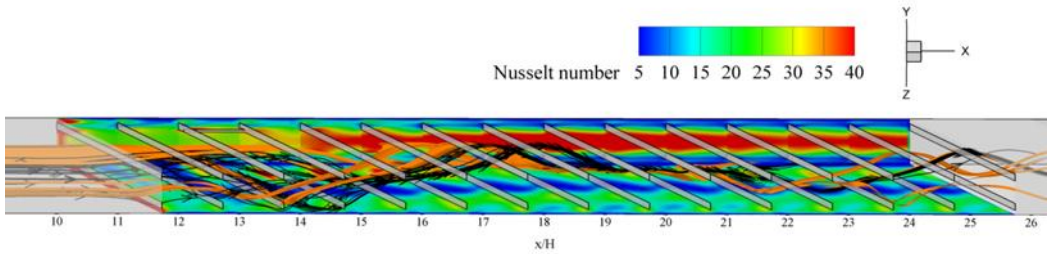

(c)

Figure 19: Streamlines impinging jet on the walls with Nu_x contours for (a)g/H = 0, (b)g/H = 0.05, and (c)g/H = 0.10 at Re = 800.

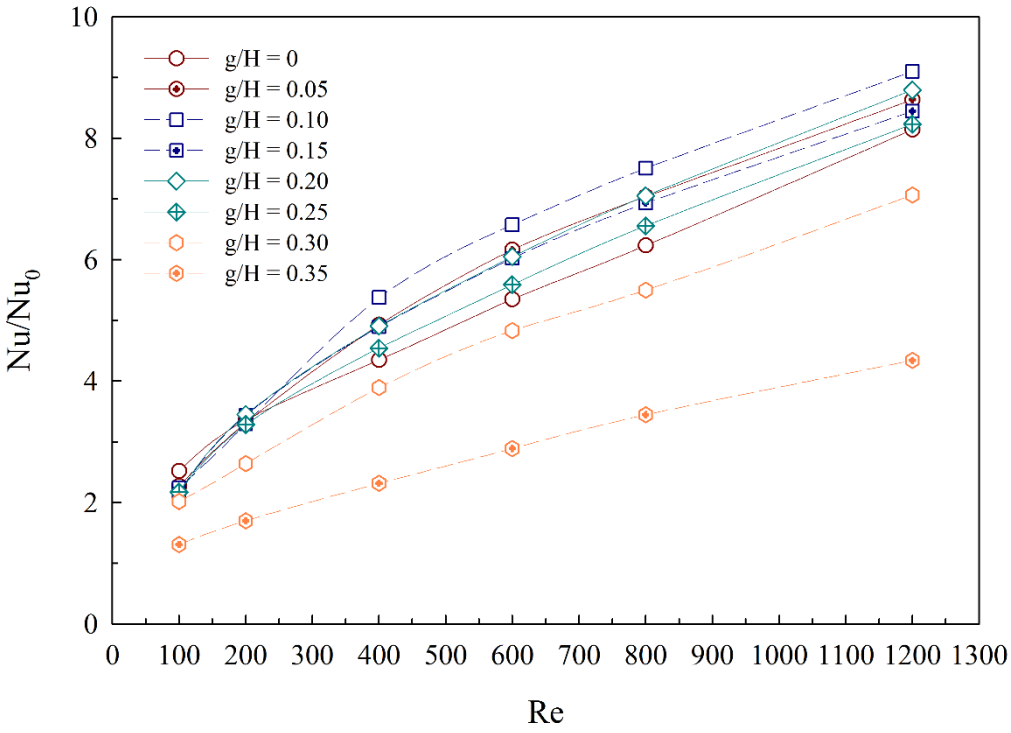

Figure 20: The variations of Nu/Nu_0 with Reynolds number.

5. CONCLUSION

3D numerical investigations for the heat transfer characteristics and performanceevaluations in a square channel with rib vortex generators, *RVG*sare presented. The effects of g/H = 0 – 0.35 values with singleblockage ratio and pitch ratio,BR = 0.15 and PR = 1 for inclined 30°*RVG*s are studied. The main finding of this investigation can be summarized as follows:

- The periodic concept of heat transfer, which presents in the form of Nu_x contours, can describe the behaviors; developing profiles and periodic profiles. The developing profiles are found at the entry regime of the test section, when passing around 6^{th} – 9^{th} moduleof the *RVG*s, the periodic profiles are appearing.

- The variations of Nu/Nu_0 at various positions indicate that the profiles of heat transfer can be divided into two regimes: periodic heat transfer profiles and fully developed periodic heat transfer profiles. Similar trends of Nu/Nu_0 are found in periodic heat transfer regimes, while the relations on both trends and values of Nu/Nu_0 are established in fully developed periodic heat transfer regimes.

- The decrease of the continuous flow area is a key to become to the fully developed periodic heat transfer profiles at the sidewallsfaster, but the upper–lower walls provide thereversed results.

- The use of the *RVG*s performs higher heat transfer rate, friction factor and the thermal performance than the smooth channelfor all cases. The augmentations are around 1 – 9 and 1.5 – 11.2 times higher than the smooth channel for heat transfer and friction factor, respectively. The *TEF* is found to be optimum around 4.05 at g/H = 0.10 and Re = 1200.

NOMENCLATURE

BR	flow blockage ratio, (b/H)
b	rib height, m
D_h	hydraulic diameter of the square channel (=H), m
H	channel height, m
f	friction factor
g	gap between upper-lower walls and *RVG*
h	convective heat transfer coefficient, W m^{-2} K^{-1}
k	thermal conductivity, W m^{-1} K^{-1}
Nu	Nusselt number
P	cyclic length of one cell (or axial pitch length, H), m
p	static pressure, Pa
Pr	Prandtl number
PR	pitch orspacing ratio, P/H
Re	Reynolds number, ($=\rho \bar{u} D_k/\mu$)
RVG	rib vortex generator
T	temperature, K
TEF	thermal enhancement factor, ($=(Nu/Nu_0) / (f/f_0)^{1/3}$)
u_i	velocity in x_i-direction, m s^{-1}
$\bar{u}$	mean velocity in channel, m s^{-1}
W	channel width =H, m
Greek symbols	
μ	dynamic viscosity, kg $s^{-1}m^{-1}$
Γ	thermal diffusivity
α	rib inclination angle or angle of attack, degree
ρ	density, kg m^{-3}
Subscript	
in	inlet
0	smooth channel
pp	pumping power

6. ACKNOWLEDGEMENT

This research was funded by King Mongkut's University of TechnologyNorth Bangkok. Contract no. KMUTNB-GEN-58-52. The author would like to thank Dr. Withada Jedsadaratanachai and Assoc. Prof. Dr.Pongjet Promvonge for thesuggestions.

7. REFERENCES

[1] W. Jedsadaratanachai, S. Suwannapan andP. Promvonge, "Numerical study of laminar heat transfer in baffled square channel with various pitches", Energy Procedia, Elsevier, vol. 9, pp. 630 – 642, 2011.

[2] S. Kwankaomeng and P. Promvonge, "Numerical prediction on laminar heat transfer in square duct with 30° angled baffle on one wall", International Communication in Heat and Mass Transfer, Elsevier,vol. 37, Issue 7, pp. 857–866, 2010.

[3] P. Promvonge, W. Jedsadaratanachai and S. Kwankaomeng,"Numerical study of laminar flow and heat transfer in square channel with 30^o inline angled baffle turbulators", Applied Thermal Engineering,Elsevier,vol. 30, Issue 11-12, pp. 1292–1303, 2010.

[4] P. Promvonge andS. Kwankaomeng,"Periodic laminar flow and heat transfer in a channel with 45° staggered V–baffles", International Communication in Heat and Mass Transfer, Elsevier, vol. 37, Issue 7, pp. 841–849, 2010.

[5] P. Promvonge, S. Sripattanapipat and S. Kwankaomeng,"Laminar periodic flow and heat transfer in square channel with 45^o inline baffles on two opposite walls", International Journal of Thermal Sciences, Elsevier,vol. 49, Issue 6, pp. 963–975, 2010.

[6] P. Promvonge, W. Jedsadaratanachai, S. Kwankaomeng and C. Thianpong,"3D simulation of laminar flow and heat transfer in V–baffled square channel",International Communication in Heat and Mass Transfer, Elsevier, vol. 39, Issue 1, pp. 85–93, 2012.

[7] A. Boonloi, "Effect of Flow Attack Angle of V-Ribs Vortex Generators in a Square Duct on Flow Structure, Heat Transfer, and Performance Improvement",Modeling and Simulation in Engineering, Hindawi,Article ID 985612, 11 pages, 2014.

[8] A. Boonloi and W. Jedsadaratanachai,"3D Numerical study on laminar forced convection in V–baffled square channel", American Journal of Applied Sciences, Science Publications, vol. 1, Issue 10, pp. 1287 – 1297, 2013.

[9] W. Jedsadaratanachai, N. Jayranaiwachira and P. Promvonge,"Computational Investigation on Fully Developed Periodic Laminar Flow Structure in Baffled Circular Tube with Various BR", Mathematical Problems in Engineering, Hindawi, Article ID 471720, 13 pages, 2014.

[10] P. Promvonge, W. Changcharoen, S. Kwankaomeng and C. Thianpong,"Numerical heat transfer study of turbulent square-duct flow through inline V-shaped discrete ribs",International Communication in Heat and Mass Transfer, Elsevier, vol. 28, Issue 10, pp.1392–1399, 2011.

[11] W. Jedsadaratanachai, "Influences of RVG positions on the periodic flow profiles",Mathematical Problems in Engineering, Hindawi, Article ID 752721, 17 pages, 2014.

[12] F. Incropera andP.D. Dewitt PD,"Introduction to heat transfer", 5^{rd} edition, John Wiley & Sons Inc, 2006.